Control of Social Withdrawal of Mice Deficient for the Autism Gene *Magel2* by Restoration of Vasopressin-Oxytocin Dialogue in Septum

Graphical abstract

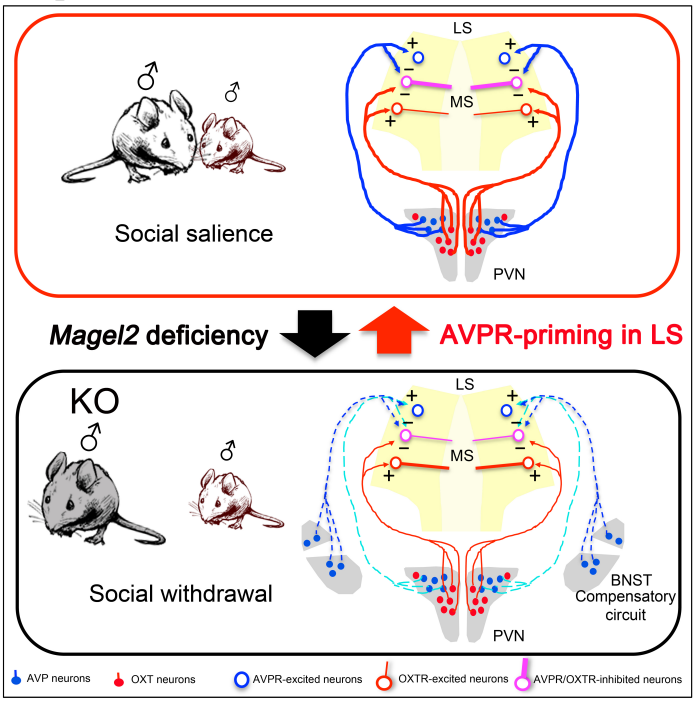

Authors

BORIE Amélie M.[1], DROMARD Yann[1], DUFNER Djodi[1], POLLOZI Emi[1], HUZARD Damien[1], TÖMBÖLI Csaba[2], OLMA Aleksandra[3], MANNING Maurice[3], COLSON Pascal[1,4], GUILLON Gilles[1], MUSCATELLI Françoise[5], DESARMÉNIEN Michel G.[1,*] & JEANNETEAU Freddy[1,*,¶]

¶Correspondance
freddy.jeanneteau@igf.cnrs.fr

In brief

Collective actions of vasopressin and oxytocin determine social salience. Borie et al. find that the degree of social novelty moderates a dialogue between networks secreting social salience hormones in the lateral septum, a region organizing sequential content of sensory experiences. Social withdrawal of mice lacking the autism gene *Magel2* is alleviated by restoration of dialogue-lead with vasopressin.

Highlights

- Social novelty activates the hypothalamoseptal vasopressin (AVP) pathway
- Social habituation activates the hypothalamoseptal oxytocin (OXT) pathway
- Disarray of AVP and OXT responses in LS mimics social disabilities of *Magel2* KO mice
- Paucity of cells detecting coincident AVP and OXT in LS of *Magel2* KO mice
- Sociability restored in *Magel2* KO mice by AVP-priming of OXT responses in LS

Author affiliation:

[1] Institut de Génomique Fonctionnelle, INSERM, CNRS, Montpellier University, France
[2] Laboratory of Chemical Biology, Biological Research Centre, Szeged, Hungary
[3] University of Toledo College of Medicine and Life Sciences, USA
[4] Department of Anesthesiology and Critical Care Medicine, Arnaud de Villeneuve Academic Hospital, Montpellier, France.
[5] Institut des Neurosciences de la Méditerranée, INSERM, Aix-Marseille University, France
* Equal contribution

Summary

Intellectual and social disabilities are common comorbidities in adolescents and adults with *Magel2* gene deficiency characterizing the Prader-Willi and Schaaf-Yang neurodevelopmental syndromes. The cellular and molecular mechanisms underlying the risk for autism in these syndromes are unexplored. Here we used *Magel2* knockout mice combined with optogenetic/pharmacological tools to characterize disease modifications in the social brain network. We find that the degree of social novelty moderates a dialogue between vasopressin and oxytocin in the lateral septum, a region organizing sequential content of sensory experiences. Social withdrawal of mice lacking *Magel2* is alleviated by restoration of dialogue-lead by vasopressin. This preclinical study identifies the collective actions of vasopressin and oxytocin in the lateral septum as a key factor in the pathophysiology.

Introduction

Autism Spectrum Disorders (ASD) affect 1 in 68 and are characterized by difficulties with communication, restrictive interests and repetitive behaviors influencing the ability to function properly (Diagnostic and Statistical Manual of Mental Disorders, 5th edition). Treatment of ASD is marginal such that management of disability-adjusted life years imposes substantial economic cost and burden on families and society[1]. Neurodevelopmental disorders characterized by mutations of chromosome 15q11-13 exhibit higher than normal risk for comorbid ASD, indicating the importance of genes in this locus for the pathophysiology[2,3]. It is a large chromosomal deletion of 15q11-13 in Prader-Willi Syndrome (PWS) and a disruption of one gene in this locus, *Magel2*, in Schaaf-Yang Syndrome (SYS) that provide respectively, 25% and 75% risk for ASD based on clinical assessment by an expert physician[2,3]. *Magel2* is a maternally imprinted, paternally expressed gene central to the pathophysiology of PWS and SYS[4], which deficiency interferes with developmental functions essential for setting multi-scale organization of the nervous system controlling muscle tone and feeding[5,6]. Common symptomatic features of PWS and SYS are hypotonia, feeding difficulties during early life, social withdrawal, intellectual and/or developmental delay[4,7,8].

Mice lacking *Magel2* gene are a good model of SYS and PWS with construct and face validity as knockout mice present hypotonia, feeding difficulties during early life and social deficits[9–11]. Treatment with oxytocin (OXT) around birth restores feeding in *Magel2* knockout (KO) mice[9] and pediatric PWS patients[12] suggesting predictive validity of this mouse model. Adult *Magel2* KO mice also present ASD-like features, such as social withdrawal ameliorated by perinatal OXT treatments[9,10].

Modulation of social behavior with OXT has been at the center of many studies[13] and it is now accepted that OXT contributes to filtering social salience signals[14]. OXT is used in numerous clinical trials[15] with promising results for the treatment of ASD. While beneficial effects were observed in PWS patients treated with OXT, these effects are age dependent[16] and not consistently found over different clinical trials[17]. Furthermore, chronic OXT treatments might be deleterious to specific aspects of social behavior[18,19]. This suggests that OXT therapy is not sufficient to treat social disabilities beyond the early postnatal critical period of neurodevelopment[20] and stresses the need to better understand the OXT system and its modulators for treating social withdrawal in the adults.

Vasopressin (AVP), a peptide sharing many features with OXT[21], is also important for the regulation of social salience and has been in the center of new clinical studies. ASD patients improved social communication upon treatment with AVP[22] as well as with antagonists of AVP receptor subtype 1a (AVPR1a)[23]. The positive outcomes of both trials demands clarity about the

mechanisms underlying AVPR responses in ASD and related diseases like PWS and SYS. We hypothesized that collective actions of OXT and AVP in the social salience brain network could explain the controversial efficacy of AVPR targeted therapies. Unfortunately, the roles of OXT and AVP have mainly been interrogated in isolation whereas combinatorial effects are anticipated[24] given that both OXT and AVP are secreted in the brain upon social encounters[25]. Here, we devised strategies to understand the dual functions of AVP and OXT during social encounters in physiological conditions and in the context of *Magel2* deficiency.

Results

Social withdrawal linked to brain theta rhythmicity defects in *Magel2*$^{+m/-p}$ mice

Brain rhythmic activity, notably theta paced, across multiple regions of the social brain network is modulated by the novelty of social stimulus and associated with cognitive and emotional behaviors in humans and rodents[26,27]. Nonetheless, socially evoked theta rhythmicity has not been studied in animal models featuring autistic-like social withdrawal like the *Magel2*$^{+m/-p}$ mice. We used a telemetric system to record the brain electroencephalogram (EEG) from wire electrodes chronically implanted atop cortex as previously described[28]. Wired animals were subjected to multiple social trials with an unfamiliar juvenile (T1 to T4) followed by the encounter with a different juvenile (T5) to discriminate between degrees of novelty of the social stimulus (**Fig. 1a**). *Magel2*$^{+m/-p}$ mice performed poorly on the discrimination task with a mouse whereas object exploration was normal compared to WT littermate controls (**Fig. 1b**). At T1, EEG power spectral density analysis showed a socially induced modulation of activity in the theta band of healthy controls that is absent in *Magel2*$^{+m/-p}$ mice (**Fig. 1c**). The effect of *Magel2*$^{+m/-p}$ was specific of social stimulus as no difference with controls was observed during trials with objects (**Fig. 1c**). Changes of socially evoked theta rhythmicity correlated with the exploration time of conspecifics in WT controls but not in *Magel2*$^{+m/-p}$ mice (**Fig. 1d**). This contrasted with theta rhythmicity in trials with objects that did not correlate with the degree of novelty in WT controls but did in *Magel2*$^{+m/-p}$ mice (**Fig. 1d**). Therefore, this behavioral paradigm is sufficiently robust in *Magel2*$^{+m/-p}$ mice to detect social exploration disabilities consistent with brain theta rhythmicity defects particularly marked during the first social encounter.

Abnormal septal oxytocinergic and vasopressinergic systems in *Magel2*$^{+m/-p}$ mice

Previously, we showed that low number of OXTR binding sites specifically in the lateral septum (LS) of *Magel2*$^{+m/-p}$ mice covariate with social withdrawal[10]. This suggests a key role for the LS and its modulation by OXT in the physiopathology. C-Fos mapping showed more robust induction in the LS after interaction with a conspecific than with an object (**Fig. S1a**), an effect validated with p-S6 as indicator of rapid signaling (**Fig. S1b**). Compared to WT controls, basal expression of c-Fos was high and less reactive to social trials particularly in the LS dorsal (LSD) of *Magel2*$^{+m/-p}$ mice (**Fig. S1c,d**). Additionally, there were fewer and shorter AVP fibers in the LSD of *Magel2*$^{+m/-p}$ mice (**Fig. S2a,b**) as well as more OXT fibers in the septum (**Fig. S2c,d**). Such genotypic differences of topological innervations in septum suggest that both OXT and AVP actions may influence sociability between mice as previously hypothesized in healthy rats[29,30].

To monitor the impact of AVP and the OXT analog agonist TGOT on theta rhythmicity, we combined bilateral intraseptal peptide injections with EEG recordings in freely moving cannulated mice (**Fig. 2a**). EEG power spectral analysis showed a trough of activity in the 4-8 Hz band and peak of activity in the 8-12 Hz band with AVP that contrasted with an opposite

effect of TGOT (**Fig. 2b**). Such changes of theta rhythmicity mimicked patterns evoked in WT mice at social trials T1 and T4, respectively (*cf.* **Fig. 1c**). Implicitly, it suggests that a deficit of septal AVP at T1 might impair social exploration similar to the effect of *Magel2* deficiency. To test this possibility, we injected an AVPR antagonist, the Manning compound (MC) into the septum at T1 or T3 to assess its influence on social behavior and theta rhythm (see methods for details about *in vivo* pharmacology). Only at T1, the blockade of AVPR with MC impaired social exploration like the effect of *Magel2* deficiency (**Fig. 2c**). Similarly, and only at T3, the blockade of OXT receptors (OXTR) by intraseptal injection of the selective antagonist Atosiban impaired social exploration like the effect of *Magel2* deficiency (**Fig. 2c**). Consistently, the blockade of septal AVPR at T1 and OXTR at T3 modified theta rhythmicity throughout the remaining trials (**Fig. 2d**). Together, social exploration correlated with theta rhythmicity in these mice unless septal AVPR and OXTR were inhibited at T1 (**Fig. 2e**) and T3 (**Fig. 2f**), respectively. Therefore, timely actions of AVPR and OXTR in septum generate a sequence of brain activity patterns aligned with the degree of novelty of the social stimulus.

Social salience depends on the AVP and OXT hypothalamoseptal circuits

To investigate timely activations of AVP and OXT neuronal networks, we first identified which cells responded throughout social trials to target their projections to LS with optogenetic constructs. We extended the initial c-Fos mapping to four brain regions containing AVP and OXT neurons: PVN, SON, BNST and LH[31–33]. AVP neurons were activated at T1 in the PVN of WT mice and in the BNST of *Magel2*$^{+m/-p}$ mice (**Fig. S3a,b**). OXT neurons were activated at T4 in the PVN of WT mice but less significantly in *Magel2*$^{+m/-p}$ mice (**Fig. S3c,d**). Thus, PVN neurons could be responsible for the release of AVP or OXT in the septum of WT mice unlike the septum of *Magel2*$^{+m/-p}$ mice that could rely on BNST neurons to secrete AVP.

To determine if the aforementioned sources of AVP and OXT modulate social behavior, we adopted an optogenetic silencing strategy. To this end, we used *Avp*-CRE and *Oxt*-CRE transgenic mice to independently target AAV virus coding for the CRE-dependent halorhodopsin (NpHR3.0-YFP) or eYFP into the PVN or BNST as indicated in **Fig. 3a**. CRE-mediated recombination was specific and efficient to express NpHR3.0-YFP either in OXT neurons of PVN or in AVP neurons of PVN or BNST (**Fig. 3b**). A prerequisite to operate as PVN-LS or BNST-LS circuits responding to social trials was that these neurons projected YFP-positive axon boutons into the septum (**Fig. S4a**). As expected, yellow light stimulation of recombinant NpHR3.0 in PVN of coronal brain slices reduced the firing rate of target neurons (**Fig. 3c**). In LS coronal slices, patch clamp recordings of predefined AVP-responding cells or TGOT-responding cells determined the impact of optogenetic manipulations specifically at axon boutons (**Fig. S4b**). Yellow light stimulation of NpHR3.0 on these cells had no effect in absence of social trials (**Fig. S4b-d**). On the contrary, blue light stimulation of ChR2-YFP (expressed with similar viral strategy) evoked responses typical of AVP in predefined AVP-responding cells in *Avp*-CRE animals (**Fig. S4e**) as well as TGOT in predefined TGOT-responding cells in *Oxt*-CRE animals (**Fig. S4f**). Importantly, blue-light evoked responses were blocked by the AVPR antagonist at AVP-responding cells, and OXTR antagonist at TGOT-responding cells. These results validated the optogenetic control of OXT or AVP releases from axon boutons in LS.

Optic fibers were chronically implanted atop LS bilaterally of WT mice to achieve light-dependent silencing of projecting axons from AVP neurons at T1 and from OXT neurons at T3. We found that yellow light stimulation of NpHR3.0 in the PVN-LS AVP pathway (**Fig. 3d** right) and the PVN-LS OXT pathway (**Fig. 3e**) impaired social exploration distinctly.

Hypothalamoseptal pathways activated timely to generate a functional sequence of AVP and OXT septal releases according to the degree of novelty of the social stimulus. In contrast, silencing of an extra-hypothalamoseptal pathway, the BNST-LS pathway failed to modify exploration through social trials (**Fig. 3d** left), highlighting remarkable specificity about AVP input source to the LS of WT mice under these behavioral conditions.

Disarray of AVP and OXT septal releases disrupted exploration of social salient stimuli

As sequential septal release of AVP and OXT is critical to express social exploration, we aimed to disrupt this orderly sequence during social trials with optogenetic stimulation of the hypothalamoseptal pathways. We used CRE-dependent ChR2-YFP or eYFP constructs delivered into the PVN or BNST of *Avp*-CRE and *Oxt*-CRE mice and induced light stimulation of LS projecting axons from the BNST-LS or PVN-LS circuits to alter the orderly sequence of AVP and OXT releases (**Fig. S5a-c**). Deficits of social exploration manifested if AVP was released at T3 instead of T1 from BNST-LS pathway and if OXT was secreted at T1 instead of T3 from PVN-LS pathway (**Fig. S5d-e**). Therefore, it is not the releases of AVP and OXT per se, but its orderly sequence aligned to the degree of social novelty that determined social exploration.

Paucity of cells responding to AVP and OXT orderly sequence in LS of *Magel2*$^{+m/-p}$ mice

Cellular targets in the LS of AVP and OXT orderly sequence remained to be explored. We used patch clamp recordings in coronal brain slices to characterize neurons in LS based on changes of firing rate upon bath application of AVP or TGOT. Half of the cells were selectively excited by AVP (type I) whereas the others were either stimulated selectively by TGOT (type II), or inhibited by both peptides (type III) (**Fig. 4a**). Retrobead anatomical tracing (**Fig. 4b**) revealed that the type II and III cells mostly, projected to the medial septum (MS). Connection between this pathway and the hippocampus[34] is known to organize sequential content of sensory experiences via theta-paced sequence of cell assemblies[35–37]. Modulation of sequential content by LS neurons may rely on inputs containing AVP from the hypothalamus, and glutamate from hippocampus[38], whereas outputs to MS are enriched with OXTR, suggesting that both peptides could act at different levels of this circuit. Electrophysiological response of the type III cells depended on the orderly sequence of AVP and TGOT contrary to the other cell types recorded. That is, AVP must be presented first to gain responsiveness to TGOT while the effect of AVP was unconditional to the order of presentation (**Fig. 4c**). These neurons also differed in terms of spontaneous activity patterns, morphology, and other electrophysiological properties (**Fig S6**).

Importantly, type III neurons were scarcer while type II neurons were denser in *Magel2*$^{+m/-p}$ mice than in WT controls (**Fig. 4d**). Such a change of proportion between cell types could depend on OXTR and AVPR dual expression. To distinguish AVPR and OXTR binding sites with cellular resolution, we synthetized d[Lys(Alexa-Fluor-647)^{8}]VP, a fluorescent peptide selective for mouse OXTR *in vitro* (**Fig. 5a**) and *in vivo* if co-injected with the competitive AVPR ligand MC (**Fig. 5b** bottom left). For a rather selective labeling of mouse AVPR(s) *in vivo*, higher dose of the fluorescent peptide was used with the competitive OXTR ligand TGOT (**Fig. 5b** bottom right). When injected in LS after social trials, d[Lys(Alexa-Fluor-647)^{8}]VP marked cells equipped with OXTR or AVPR, some of which also contained the activity-dependent indicator p-S6 and retrobeads (**Fig. 5c**). Specifically, LS cells projecting to MS were more abundant and more responsive to social trials in WT controls than in *Magel2*$^{+m/-p}$ mice (**Fig. 5d,e**). These cells are mostly GABAergic somatostatin neurons labelled with retrobeads

(likely the type III, **Fig. S7**). All in all, the septum of *Magel2*$^{+m/-p}$ mice is ill equipped to organize sequential content of social signals evoked by AVP and OXT releases (**Fig. 5f**).

AVPR priming in LS of *Magel2*$^{+m/-p}$ mice restored exploration of social salient stimuli

To normalize theta-paced sequence of cell assemblies in the LS of *Magel2*$^{+m/-p}$ mice, we promoted AVPR septal response during the first social encounter (**Fig. S8d**). For this, *Magel2*$^{+m/-p}$ mice were cannulated in LS to receive bilateral AVP injections at T1, which increased theta rhythmicity throughout trials (**Fig. S8a**) and restored social exploration (**Fig. 6a**). These activities were not correlated if NaCl or AVP+Atosiban were injected instead of AVP alone (**Fig. 6b** and methods for details about *in vivo* pharmacology). Consistently, NaCl or AVP+Atosiban injections failed to restore theta rhythmicity and social exploration (**Fig. 6a**, **S8a**). Thus, inhibition of septal OXTR with Atosiban despite AVPR priming highlighted the necessity of AVPR and OXTR collective responses to restore social behavior of *Magel2*$^{+m/-p}$ mice.

In a second experiment, we promoted the OXT system of *Magel2*$^{+m/-p}$ mice given its clinical potential for alleviating social disabilities in humans[39,40]. To this end, we used optogenetic stimulation of CRE-dependent ChR2-YFP recombined in OXT neurons of PVN in *Oxt*-CRE x *Magel2*$^{+m/-p}$ mice to promote OXT septal release during social habituation. This manipulation increased exploration duration with known and unknown mice without discrimination (**Fig. 6c**), and exploration duration correlated with changes of theta rhythmicity (**Fig. 6d**). Theta rhythm of *Magel2*$^{+m/-p}$ mice optogenetically-stimulated for OXT septal release (**Fig. S8b**) looks alike that of WT mice optogenetically-deprived of AVPR septal response at T1 (**Fig. 2d**). Thus, OXT therapies may not be optimally effective in diseases characterized by AVPR sequential priming defects.

In a third experiment, we used optogenetic stimulation of ChR2-YFP recombined in AVP neurons of PVN or BNST of *Avp*-CRE x *Magel2*$^{+m/-p}$ mice to simulate AVP release normally evoked by the first social encounter. We found that blue light-stimulation of the BNST-LS AVP pathway promoted consistent social exploration (**Fig. 6e** right) unlike stimulation of the PVN-LS AVP pathway (**Fig. 6e** left). Optogenetic stimulation of BNST-LS AVP terminals of *Magel2*$^{+m/-p}$ mice modulated theta rhythmicity (**Fig. S8c**) that correlated with social exploration (**Fig. 6f**). This result indicates that social behavior is restored in *Magel2*$^{+m/-p}$ mice by promoting AVPR septal response during the first encounter through the BNST-LS AVP pathway.

Collectively, one promising avenue for disease modification is to restore the orderly sequence of AVP and OXT responses for organizing theta-paced sequence of social salient information flow through the septum.

Discussion

One major feature of physiopathology associated with *Magel2* deficiency reported in this study is the abnormal functional topology of both the AVP and OXT neuronal networks innervating the septum. This is decisive because AVP and OXT must act collectively on septal neurons to demonstrate social salience. Normally, AVP acts first on septal neurons upon release evoked by the novelty of the social stimulus while OXT acts second on septal neurons upon release elicited by the repetition of the social stimulus as previously suggested in rats[41,42]. It is the degree of social novelty that commanded sequential activations of AVP and OXT hypothalamoseptal neuronal networks as seen with the c-Fos mapping studies.

Pathologically, not only septal AVP fibers were scarcer and PVN AVP neurons poorly activated upon social novelty but also a cryptic extra-hypothalamoseptal AVP network originating from the BNST was activated by social encounters. This suggested that a functional map-to-action relevant for expressing sequential content as described in the hippocampus[36] could differ between *Magel2*$^{+m/-p}$ mice and WT controls for perceiving the degree of social novelty. Perhaps, new social encounters are seen as threatening more than rewarding by *Magel2*$^{+m/-p}$ mice, resulting in the mobilization of alternate circuit pathways that influence behavioral response. For instance, threats, unpredictability and social anxiety activate the BNST in which the lesion of AVP cells specifically, reduced social anxiety and aggressiveness[43,44]. Many brain regions among which the PVN and BNST induced *c-Fos* and either *Oxtr* or *Avpr(s)* if conspecific odors came from healthy individuals or sick individuals, respectively. Further blockade of AVPR inhibited social avoidance to sick odors[45], thus providing evidence that socially evoked activation of AVP BNST cells is an appropriate response to threats that *Magel2*$^{+m/-p}$ mice may privilege even with healthy conspecific. In fact, activation of LSD neurons, a region rich of AVP fibers, inhibits aggressive behavior in mice via its projections to the ventromedial hypothalamus[46]. In *Magel2*$^{+m/-p}$ mice, c-Fos activation was elevated in all septal areas under isolation, failing to respond upon social encounters unlike healthy controls, indicating a possible conflict between social perception and theta paced neuronal activation in the social brain network[27]. Despite their social disabilities, *Magel2*$^{+m/-p}$ mice perform well with object exploration, exhibiting correlated activities with theta rhythmicity. This contrasts with the WT mice that did not show such correlated activities in the object trials. In agreement, the sensitivity for discriminating faces and objects was reported respectively, impaired and enhanced in adolescents with ASD[47] which adds to the face validity of the *Magel2*$^{+m/-p}$ mice as model of ASD.

Abnormalities in the OXT PVN-LS pathway were less prominent than in the AVP system of *Magel2*$^{+m/-p}$ mice. This is surprising considering the alteration of oxytocinergic neurons function described in *Magel2*$^{+m/-p}$ mice[48] but could be due to compensatory mechanisms on post-synaptic target cells in the LSD such as the replacement of type III neurons by the type II or such as the increase of OXT fibers in the LS. Besides the apparent disarray between AVP and OXT septal releases in *Magel2*$^{+m/-p}$ mice, abnormal septal response to social salience hormones corresponded to the underrepresentation of type III neurons belonging to the LS-MS pathway previously described as sequence generator linked with the hippocampus[37,49]. These neurons, which are unconditionally inhibited by AVPR, must gain competence to be inhibited by OXTR thereby operating as detectors of coincidence organizing the orderly sequence of AVP and OXT septal response within a functional map-to-action. Despite the septum of *Magel2*$^{+m/-p}$ mice is ill equipped, promoting AVPR septal response during social novelty restored social behavior more efficiently than by stimulation of OXTR septal response during social habituation. Therefore, restoring a complete orderly sequence of AVPR and OXTR septal releases is essential for organizing sequential content of social salience signals. This mechanism could also have implications for treating human pathologies given that activity of the hypothalamoseptal areas was associated with affiliative emotion[50], and that OXT given intranasally increases the functional connectivity between the septum and other key areas of the social salience and reward circuits[51].

Therapeutic priming of AVPR septal response for a few minutes at the time of social novelty restored social discrimination more than 1h later by a mechanism requiring OXTR septal response in *Magel2*$^{+m/-p}$ mice. Molecular and electrophysiological studies provided some clues to understand this effect. First, AVP-deficient Bratteleboro rats centrally administered

with AVP corrected for several hours the frequency deficit of theta rhythm[52]. Second, AVPR and OXTR responses overlap in the septum where theta paced sequence of cells assemblies projecting to the hippocampus are modulated by OXT and AVP[53]. Third, sequential content of AVP and OXT in septum is suspected to modify theta paced network activity during social encounter. Consistent with an AVPR priming effect in the LS, AVP stimulation of LS neurons was previously shown to condition subsequent excitatory response to glutamatergic inputs from the hippocampus in rats[54,55]. Fourth, cells detecting the coincidence of AVP and OXT sequential content are underrepresented in septum of *Magel2*$^{+m/-p}$ mice. They are GABAergic somatostatin-positive cells (type III) projecting to MS likely equipped with both AVPR and OXTR. Unfortunately, this remains an open question, as d[Lys(Alexa-Fluor-647)^{8}]VP did not allow for co-labeling of OXTR and AVPR. Lack of AVPR priming during social novelty impaired theta paced information flow through the septum to express social salience by OXTR modulation during habituation. So, therapeutic AVPR priming of *Magel2*$^{+m/-p}$ mice should restore septal network activity in response to social encounter. Consistently, intranasal administration of AVP (but not OXT) increased reciprocated collaboration between humans and its associated reactivity in the LS[56] even several days beyond treatment[57].

In terms of clinical perspectives, it is encouraging that priming of septal AVPR can be achieved even by a cryptic source of AVP (*e.g.* the BNST-LS pathway), further illustrating that circuit defects can be alleviated by loading the septum with AVP at the right time. Moreover, theta paced septal activity and its modulation by social salience hormones is an opportunity to use EEG recordings for predicting social behavior outcomes as demonstrated in this study and others[27]. In humans, EEG abnormalities and epilepsy have been reported in patients with PWS[58] and ASD[59]. Few studies reported deficits of social task-related EEG power spectrum changes in ASD patients[60,61]. Here, we provide not only an EEG signature of social disabilities in *Magel2*$^{+m/-p}$ mice but also a blueprint of traces specific for AVPR and OXTR modulations in mouse septum corroborated in rats[53]. Future research will focus on improving an EEG predictive marker of the sensitivity to AVP and OXT in related pathologies and therapies. This is particularly relevant in pathologies such as PWS, SYS and ASD because of the heterogeneity of clinical features and the responses to treatments (*e.g.* bumetamide[62] and oxytocin[63]).

CONTRIBUTIONS

A.M.B, M.G.D and F.J designed and verified analytical methods. A.M.B, Y.D, D.D and D.H carried behavior studies. A.M.B, M.G.D carried electrophysiological studies. A.M.B and Y.D carried stereotaxic injections. Cs.T, A.O and M.M synthesized d[Lys(Alexa-Fluor-647)^{8}]VP, characterized *in vitro* by G.G and *in vivo* by F.J and Y.D. E.P performed histology. D.D and E.P verified implantations in postmortem brains. A.M.B and D.D analyzed EEG. F.M and P.C provided critical feedback. A.M.B and F.J wrote the manuscript. All authors reviewed and approved the final manuscript. The authors declare no competing financial interests.

ACKNOWLEDGEMENTS

This work is supported by ANR (M.G.D, F.M), Fondation Lejeune (M.G.D), Fondation pour la recherche médicale (F.J, A.M.B), Centre hospitalier de Montpellier (D.D., P.C.), Montpellier University (A.M.B), and generous support from R. Makineni, R. Tyner, F. Paulsen (M.M.). We thank from IGF in Montpellier, N. Marchi for sharing EEG devices, B. Boussadia for advices on EEG, M. Arango-Lievano for technical strategies, critical reading of the manuscript and M. Tauber (CHU Toulouse) for discussions on PWS.

ABBREVIATIONS

AAV, Adeno-associated virus; ASD, Autism spectrum disorder; Ato, Atosiban; AVP, Arginine-Vasopressin; AVPR, AVP receptor; BNST, Bed stria terminalis nucleus; ChR2, Channel rhodopsin-2; EEG, electroencephalogram; GABA, gamma-aminobutyric acid; GLU, glutamate; KO, Knockout; LH, Lateral hypothalamus; LS, Lateral septum; LSD, LS dorsal; LSI, LS intermediate; LSV, LS ventral; Magel2, MAGE family member L2; MC, Manning Compound; MS, Medial septum; NpHR3, Halorhodopsin-3; OXT, Oxytocin; OXTR, OXT receptor; PVN, Paraventricular nucleus; PWS, Prader-Willi Syndrome; p-S6, phospho-protein ribosomal S6; SON, Supraoptic nucleus; SYS, Schaaf-Yang syndrome; WT, wildtype; YFP, Yellow protein fluorescent.

REFERENCES

1. Masi, A., DeMayo, M. M., Glozier, N. & Guastella, A. J. An Overview of Autism Spectrum Disorder, Heterogeneity and Treatment Options. *Neurosci. Bull.* **33**, 183–193 (2017).
2. Dykens, E. M., Lee, E. & Roof, E. Prader–Willi syndrome and autism spectrum disorders: an evolving story. *J. Neurodev. Disord.* **3**, 225–237 (2011).
3. Schaaf, C. P. *et al.* Truncating mutations of MAGEL2 cause Prader-Willi phenotypes and autism. *Nat. Genet.* **45**, 1405–1408 (2013).
4. Fountain, M. D. & Schaaf, C. P. Prader-Willi Syndrome and Schaaf-Yang Syndrome: Neurodevelopmental Diseases Intersecting at the MAGEL2 Gene. *Diseases* **4**, (2016).
5. Kamaludin, A. A. *et al.* Muscle dysfunction caused by loss of Magel2 in a mouse model of Prader-Willi and Schaaf-Yang syndromes. *Hum. Mol. Genet.* **25**, 3798–3809 (2016).
6. Maillard, J. *et al.* Loss of Magel2 impairs the development of hypothalamic Anorexigenic circuits. *Hum. Mol. Genet.* **25**, 3208–3215 (2016).
7. Fountain, M. D. *et al.* The phenotypic spectrum of Schaaf-Yang syndrome – 18 new affected individuals from 14 families. *Genet. Med. Off. J. Am. Coll. Med. Genet.* **19**, 45–52 (2017).
8. Angulo, M. A., Butler, M. G. & Cataletto, M. E. Prader-Willi syndrome: a review of clinical, genetic, and endocrine findings. *J. Endocrinol. Invest.* **38**, 1249–1263 (2015).
9. Schaller, F. *et al.* A single postnatal injection of oxytocin rescues the lethal feeding behaviour in mouse newborns deficient for the imprinted Magel2 gene. *Hum. Mol. Genet.* **19**, 4895–4905 (2010).
10. Meziane, H. *et al.* An Early Postnatal Oxytocin Treatment Prevents Social and Learning Deficits in Adult Mice Deficient for Magel2, a Gene Involved in Prader-Willi Syndrome and Autism. *Biol. Psychiatry* **78**, 85–94 (2015).
11. Fountain, M. D., Tao, H., Chen, C.-A., Yin, J. & Schaaf, C. P. Magel2 knockout mice manifest altered social phenotypes and a deficit in preference for social novelty. *Genes Brain Behav.* **16**, 592–600 (2017).
12. Tauber, M. *et al.* The Use of Oxytocin to Improve Feeding and Social Skills in Infants With Prader-Willi Syndrome. *Pediatrics* (2017). doi:10.1542/peds.2016-2976
13. Marlin, B. J. & Froemke, R. C. Oxytocin modulation of neural circuits for social behavior. *Dev. Neurobiol.* **77**, 169–189 (2017).
14. Shamay-Tsoory, S. G. & Abu-Akel, A. The Social Salience Hypothesis of Oxytocin. *Biol. Psychiatry* **79**, 194–202 (2016).
15. Kendrick, K. M., Guastella, A. J. & Becker, B. Overview of Human Oxytocin Research. in *Behavioral Pharmacology of Neuropeptides: Oxytocin* (eds. Hurlemann, R. & Grinevich, V.) 321–348 (Springer International Publishing, 2018). doi:10.1007/7854_2017_19
16. Kuppens, R. J., Donze, S. H. & Hokken-Koelega, A. C. S. Promising effects of oxytocin on social and food-related behavior in young children with Prader-Willi Syndrome: a randomized, double-blind, controlled crossover trial. *Clin. Endocrinol. (Oxf.)* (2016). doi:10.1111/cen.13169
17. Rice, L. J., Einfeld, S. L., Hu, N. & Carter, C. S. A review of clinical trials of oxytocin in Prader-Willi syndrome. *Curr. Opin. Psychiatry* **31**, 123–127 (2018).
18. Bales, K. L. *et al.* Chronic intranasal oxytocin causes long-term impairments in partner preference formation in male prairie voles. *Biol. Psychiatry* **74**, 180–188 (2013).
19. Huang, H. *et al.* Chronic and Acute Intranasal Oxytocin Produce Divergent Social Effects in Mice. *Neuropsychopharmacol. Off. Publ. Am. Coll. Neuropsychopharmacol.* (2013). doi:10.1038/npp.2013.310
20. Muscatelli, F., Desarménien, M. G., Matarazzo, V. & Grinevich, V. Oxytocin Signaling in the Early Life of Mammals: Link to Neurodevelopmental Disorders Associated with ASD. *Curr. Top. Behav. Neurosci.* **35**, 239–268 (2018).

21. Song, Z. & Albers, H. E. Cross-talk among oxytocin and arginine-vasopressin receptors: Relevance for basic and clinical studies of the brain and periphery. *Front. Neuroendocrinol.* (2017). doi:10.1016/j.yfrne.2017.10.004
22. Parker, K. J. *et al.* A randomized placebo-controlled pilot trial shows that intranasal vasopressin improves social deficits in children with autism. *Sci. Transl. Med.* eaau7356 (2019). doi:10.1126/scitranslmed.aau7356
23. Bolognani, F. *et al.* A phase 2 clinical trial of a vasopressin V1a receptor antagonist shows improved adaptive behaviors in men with autism spectrum disorder. *Sci. Transl. Med.* eaat7838 (2019). doi:10.1126/scitranslmed.aat7838
24. Carter, C. S. The Oxytocin–Vasopressin Pathway in the Context of Love and Fear. *Front. Endocrinol.* **8**, (2017).
25. Veenema, A. H. & Neumann, I. D. Central vasopressin and oxytocin release: regulation of complex social behaviours. *Prog. Brain Res.* **170**, 261–276 (2008).
26. Korotkova, T. *et al.* Reconciling the different faces of hippocampal theta: The role of theta oscillations in cognitive, emotional and innate behaviors. *Neurosci. Biobehav. Rev.* **85**, 65–80 (2018).
27. Tendler, A. & Wagner, S. Different types of theta rhythmicity are induced by social and fearful stimuli in a network associated with social memory. *eLife* **4**, (2015).
28. Arango-Lievano, M. *et al.* Topographic Reorganization of Cerebrovascular Mural Cells under Seizure Conditions. *Cell Rep.* **23**, 1045–1059 (2018).
29. Landgraf, R. *et al.* V1 vasopressin receptor antisense oligodeoxynucleotide into septum reduces vasopressin binding, social discrimination abilities, and anxiety-related behavior in rats. *J. Neurosci. Off. J. Soc. Neurosci.* **15**, 4250–4258 (1995).
30. Menon, R. *et al.* Oxytocin Signaling in the Lateral Septum Prevents Social Fear during Lactation. *Curr. Biol. CB* **28**, 1066-1078.e6 (2018).
31. Grinevich, V., Knobloch-Bollmann, H. S., Eliava, M., Busnelli, M. & Chini, B. Assembling the Puzzle: Pathways of Oxytocin Signaling in the Brain. *Biol. Psychiatry* **79**, 155–164 (2016).
32. Rood, B. D. & De Vries, G. J. Vasopressin innervation of the mouse (Mus musculus) brain and spinal cord. *J. Comp. Neurol.* **519**, 2434–2474 (2011).
33. Sukhov, R. R., Walker, L. C., Rance, N. E., Price, D. L. & Young, W. S. Vasopressin and oxytocin gene expression in the human hypothalamus. *J. Comp. Neurol.* **337**, 295–306 (1993).
34. Leranth, C. & Frotscher, M. Organization of the septal region in the rat brain: cholinergic-GABAergic interconnections and the termination of hippocampo-septal fibers. *J. Comp. Neurol.* **289**, 304–314 (1989).
35. Bender, F. *et al.* Theta oscillations regulate the speed of locomotion via a hippocampus to lateral septum pathway. *Nat. Commun.* **6**, 8521 (2015).
36. Buzsáki, G. & Tingley, D. Space and Time: The Hippocampus as a Sequence Generator. *Trends Cogn. Sci.* **22**, 853–869 (2018).
37. Tsanov, M. Differential and complementary roles of medial and lateral septum in the orchestration of limbic oscillations and signal integration. *Eur. J. Neurosci.* **48**, 2783–2794 (2018).
38. Jakab, R. L., Naftolin, F. & Leranth, C. Convergent vasopressinergic and hippocampal input onto somatospiny neurons of the rat lateral septal area. *Neuroscience* **40**, 413–421 (1991).
39. Benner, S. & Yamasue, H. Clinical potential of oxytocin in autism spectrum disorder: current issues and future perspectives. *Behav. Pharmacol.* **29**, 1–12 (2018).
40. Kabasakalian, A., Ferretti, C. J. & Hollander, E. Oxytocin and Prader-Willi Syndrome. *Curr. Top. Behav. Neurosci.* **35**, 529–557 (2018).
41. Lukas, M., Toth, I., Veenema, A. H. & Neumann, I. D. Oxytocin mediates rodent social memory within the lateral septum and the medial amygdala depending on the relevance of the social stimulus: male juvenile versus female adult conspecifics. *Psychoneuroendocrinology* **38**, 916–926 (2013).
42. Lukas, M., Bredewold, R., Landgraf, R., Neumann, I. D. & Veenema, A. H. Early life stress impairs social recognition due to a blunted response of vasopressin release within the septum of adult male rats. *Psychoneuroendocrinology* **36**, 843–853 (2011).
43. Clauss, J. A., Avery, S. N., Benningfield, M. M. & Blackford, J. U. Social anxiety is associated with BNST response to unpredictability. *Depress. Anxiety* (2019). doi:10.1002/da.22891
44. Rigney, N., Whylings, J., Mieda, M., de Vries, G. J. & Petrulis, A. Sexually Dimorphic Vasopressin Cells Modulate Social Investigation and Communication in Sex-Specific Ways. *eNeuro* **6**, (2019).
45. Arakawa, H., Arakawa, K. & Deak, T. Oxytocin and vasopressin in the medial amygdala differentially modulate approach and avoidance behavior toward illness-related social odor. *Neuroscience* **171**, 1141–1151 (2010).

46. Wong, L. C. *et al.* Effective Modulation of Male Aggression through Lateral Septum to Medial Hypothalamus Projection. *Curr. Biol. CB* **26**, 593–604 (2016).
47. Pallett, P. M., Cohen, S. J. & Dobkins, K. R. Face and Object Discrimination in Autism, and Relationship to IQ and Age. *J. Autism Dev. Disord.* **44**, 1039–1054 (2014).
48. Ates, T. *et al.* Inactivation of Magel2 suppresses oxytocin neurons through synaptic excitation-inhibition imbalance. *Neurobiol. Dis.* **121**, 58–64 (2019).
49. Deng, K. *et al.* Whole-brain mapping of projection from mouse lateral septal nucleus. *Biol. Open* **8**, bio043554 (2019).
50. Moll, J. *et al.* A neural signature of affiliative emotion in the human septohypothalamic area. *J. Neurosci. Off. J. Soc. Neurosci.* **32**, 12499–12505 (2012).
51. Rilling, J. K., Chen, X., Chen, X. & Haroon, E. Intranasal oxytocin modulates neural functional connectivity during human social interaction. *Am. J. Primatol.* **80**, e22740 (2018).
52. Urban, I. J. Effects of vasopressin and related peptides on neurons of the rat lateral septum and ventral hippocampus. *Prog. Brain Res.* **119**, 285–310 (1998).
53. Urban, I. J. Intraseptal administration of vasopressin and oxytocin affects hippocampal electroencephalogram in rats. *Exp. Neurol.* **74**, 131–147 (1981).
54. Urban, I. J. & De Wied, D. Effect of vasopressin, oxytocin and peptides derived from these hormones on field potential induced in lateral septum of rats by stimulation of the fimbria fornix. *Neuropeptides* **7**, 41–49 (1986).
55. Van den Hooff, P. & Urban, I. J. Vasopressin facilitates excitatory transmission in slices of the rat dorso-lateral septum. *Synap. N. Y. N* **5**, 201–206 (1990).
56. Rilling, J. K. *et al.* Effects of intranasal oxytocin and vasopressin on cooperative behavior and associated brain activity in men. *Psychoneuroendocrinology* **37**, 447–461 (2012).
57. Rilling, J. K. *et al.* Arginine Vasopressin Effects on Subjective Judgments and Neural Responses to Same and Other-Sex Faces in Men and Women. *Front. Endocrinol.* **8**, (2017).
58. Verrotti, A., Soldani, C., Laino, D., d'Alonzo, R. & Grosso, S. Epilepsy in Prader-Willi syndrome: clinical, diagnostic and treatment aspects. *World J. Pediatr. WJP* **10**, 108–113 (2014).
59. El Achkar, C. M. & Spence, S. J. Clinical characteristics of children and young adults with co-occurring autism spectrum disorder and epilepsy. *Epilepsy Behav. EB* **47**, 183–190 (2015).
60. Oberman, L. M. *et al.* EEG evidence for mirror neuron dysfunction in autism spectrum disorders. *Cogn. Brain Res.* **24**, 190–198 (2005).
61. Castelhano, J., Tavares, P., Mouga, S., Oliveira, G. & Castelo-Branco, M. Stimulus dependent neural oscillatory patterns show reliable statistical identification of autism spectrum disorder in a face perceptual decision task. *Clin. Neurophysiol. Off. J. Int. Fed. Clin. Neurophysiol.* **129**, 981–989 (2018).
62. Lemonnier, E. *et al.* Effects of bumetanide on neurobehavioral function in children and adolescents with autism spectrum disorders. *Transl. Psychiatry* **7**, e1056 (2017).
63. Parker, K. J. *et al.* Intranasal oxytocin treatment for social deficits and biomarkers of response in children with autism. *Proc. Natl. Acad. Sci. U. S. A.* **114**, 8119–8124 (2017).

FIGURE LEGENDS

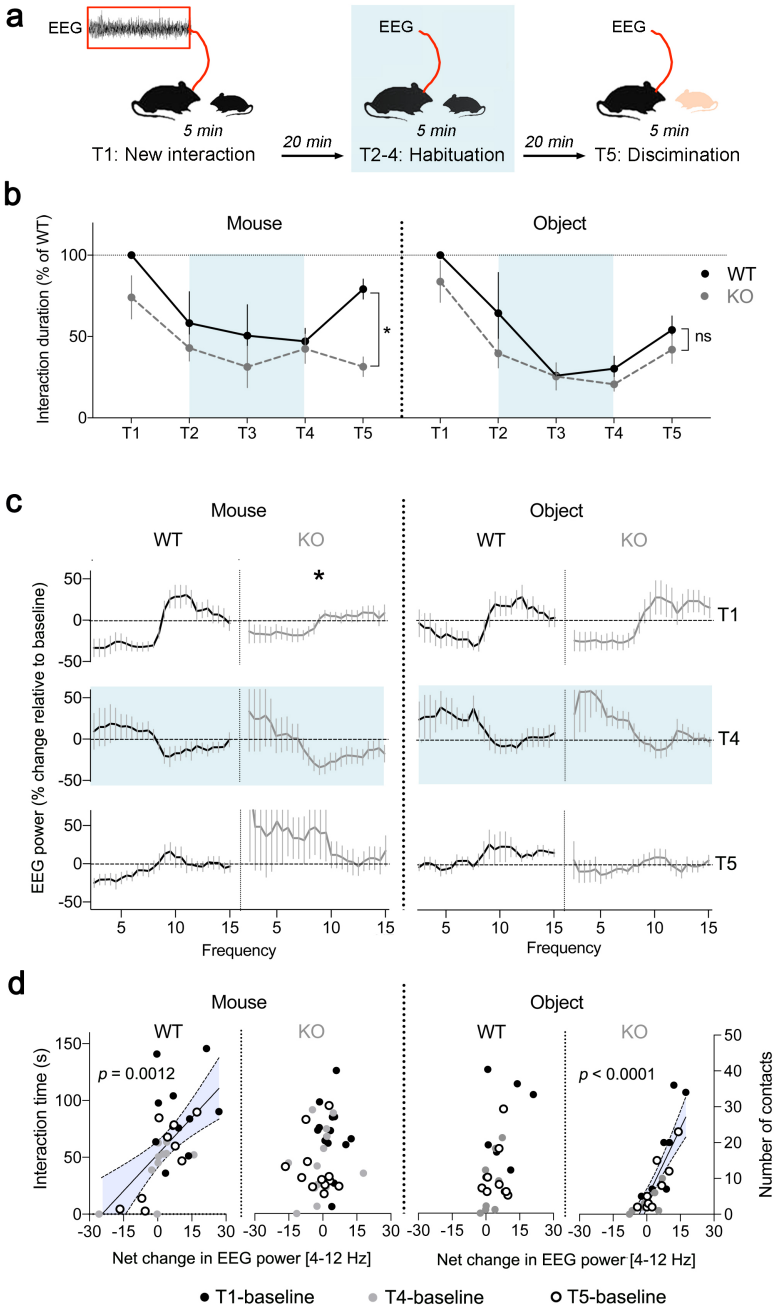

Figure 1. Deficits of EEG theta activity correlated with social defects in *Magel2*$^{+m/-p}$ mice.

(**a**) Experimental timeline: EEG recorded during social habituation with a juvenile in 4 successive trials (T1-T4) of 5 min followed by a 5th trial (T5) with a new conspecific.

(**b**) Time exploring a mouse (left) or an object (right) throughout trials. Data (means±SEM) expressed as % of WT in n=15WT, 16KO mice for social and n=13WT, 15KO for non-social tests. Two-way ANOVA for social test: effect of trials $p<0.0001$, genotype $p=0.028$, and interaction $p=0.035$, post-hoc Sidak test comparing WT and KO at T5 *$p<0.0001$. For non-social test: effect of trials $p<0.0001$, genotype $p=0.14$, and interaction $p=0.71$.

(**c**) Change in EEG power spectrum during trials. Data (means±SEM) expressed as % relative to baseline in n=11WT, 13KO mice for social and n=8WT, 8KO for non-social tests. Two-way ANOVA for social test: effect of

genotype on the theta band at T1 $p<0.0001$, post-hoc Sidak test *$p<0.05$; at T4 $p>0.9$; at T5 $p=0.009$. For non-social test: no effect of genotype on the theta band.

(**d**) Net changes of EEG power in the theta band during trials correlated with behavioral performance. For social test (interaction time in seconds): Spearman coefficient in WT $r=0.56$, $p=0.0012$ and KO $r=0.21$, $p=0.18$. For non-social test (number of contact with object): Spearman coefficient in WT $r=0.39$, $p=0.053$ and KO $r=0.85$, $p<0.0001$.

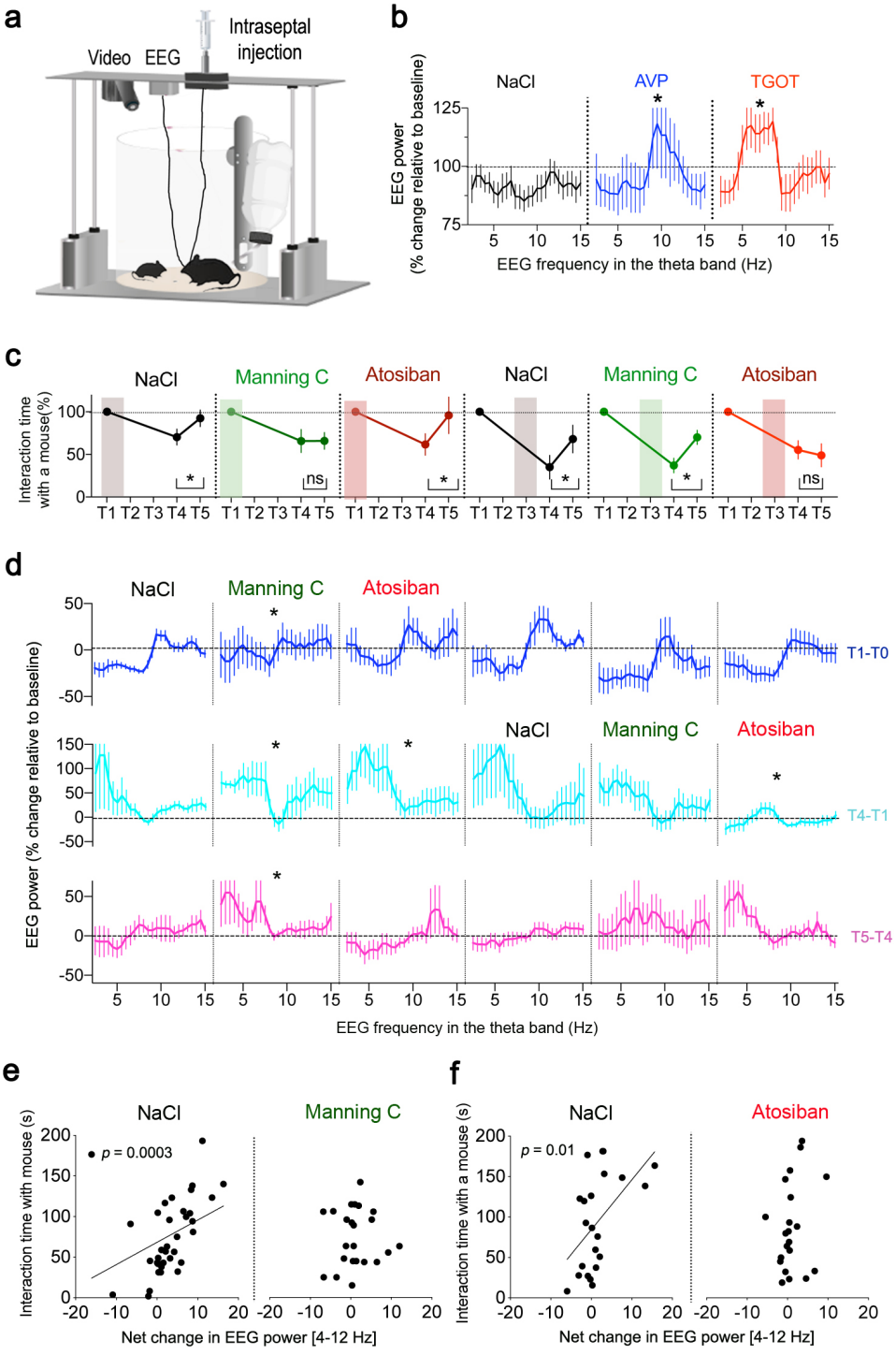

Figure 2. AVP and OXT receptors in septum modulate EEG theta rhythm during social behavior.
(**a**) Experimental setup to inject drugs in cannulated septum while recording EEG in freely moving mice.
(**b**) Percent change of EEG power in the low theta band [4-8 Hz] after intraseptal-injection of TGOT (3.10^{-6} M for 9 min) and in the high theta band [8-12 Hz] with AVP (3.10^{-5} M for 9 min). Means±SEM of n=13 NaCl, 10 AVP, 10 TGOT at 10 min post-injection: Kruskal Wallis test p=0.0011, effect of AVP *p=0.04 and TGOT *p=0.0005.
(**c**) Time exploring a mouse throughout trials upon intra-septal injection of Manning Compound (10^{-8} M), atosiban (10^{-8} M) or vehicle at T1 or T3. Data (means±SEM) expressed as % relative to T1 in n=16 NaCL, 9 MC, 9 Atosiban

mice injected at T1 and n=8 NaCL, 8 MC, 8 Atosiban mice injected at T3. Two-way ANOVA: effect of trials $p<0.0001$, post-hoc Dunnett test comparing T4 and T5 for NaCl $*p=0.042$, for Atosiban $*p=0.023$. Two-way ANOVA: effect of trials $p<0.0001$, post-hoc Dunnett test comparing T4 and T5 for NaCl $*p=0.0017$, for MC $*p=0.0048$. See the methods for the selectivity of MC and Atosiban on mOXTR and mAVPR.

(**d**) Change of EEG power spectrum at T1 (top), T4 (middle) and T5 (bottom). Effect of intraseptal-injections at T1 of vehicle (NaCl), Manning C (MC 10^{-8} M) or atosiban (Ato 10^{-8} M). Data (means±SEM) expressed as % relative to baseline in n=11 NaCl, 8 MC, 7 Ato mice: Kruskal Wallis test at T1 $p=0.021$, effect of MC $*p=0.0158$; at T4 $p=0.0015$, effect of MC $*p=0.0052$ and Ato $*p=0.0026$; at T5 $p<0.0001$, effect of MC $*p=0.007$. Effect of intraseptal-injections at T3. Means±SEM of N=8 NaCl, 7 MC, 9 Ato mice: Kruskal Wallis test at T4 $p<0.0001$, effect of Ato $*p<0.0001$; at T5 $p=0.0003$, effect of Ato $*p=0.0028$.

(**e**) Net changes of EEG power in the theta band between trials and baseline correlated with the interaction time with a mouse. Spearman coefficient if NaCl injected at T1: $r=0.56$, $p=0.0003$; if MC injected at T1: $r = 0.03$, $p=0.86$.

(**f**) Net changes of EEG power in the theta band between trials and baseline correlated with the interaction time with a mouse. Spearman coefficient if NaCl injected at T3 $r=0.53$, $p=0.01$; if Ato injected at T3 $r=0.3$, $p=0.17$.

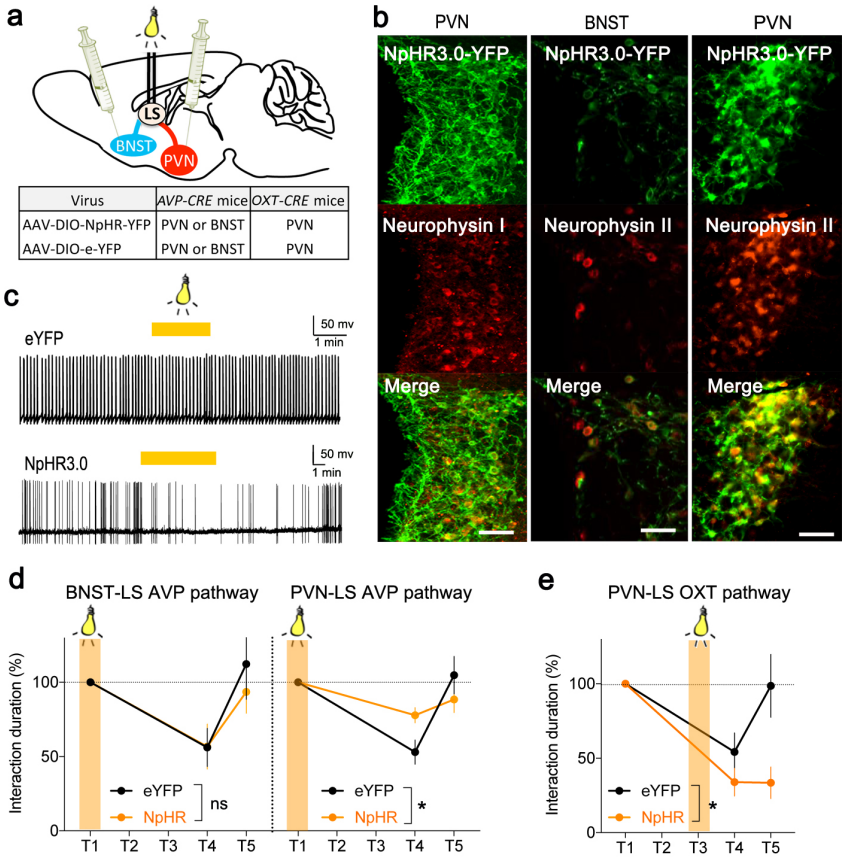

Figure 3. Modulation of social behavior by optogenetic inhibition of the OXT and AVP septohypothalamic circuit pathways.

(**a**) Viral-mediated optogenetic silencing of septal inputs from OXT neurons (*Oxt*-CRE mice) in hypothalamic paraventricular nucleus (PVN) or from AVP neurons (*Avp*-CRE mice) in PVN or Bed nucleus of stria terminalis (BNST).

(**b**) Co-expression of CRE-mediated NpHR3.0-YFP with Neurophysin I (OXT) in PVN neurons or with Neurophysin II (AVP) in PVN as well as BNST neurons. Scale=25 µm.

(**c**) Firing of action potentials recorded in whole cell configuration in OXT neurons expressing NpHR3.0-YFP or eYFP. Stimulation of cell body with yellow light decreased firing rate.

(**d**) Time exploring a mouse throughout trials. Data (means±SEM) expressed as % relative to T1 in each group of n=8 eYFP, 9 NpHR3.0 in BNST and 11 eYFP, 10 NpHR3.0 in PVN of *Avp-CRE* mice. Two-way ANOVA: Interaction of trials and NpHR3.0 stimulation with light (561nm, continuous stimulation, 5min, ~2mW at T1) of BNST fibers: p=0.6; of PVN fibers: p=0.01 post-hoc Sidak test comparing eYFP with NpHR3.0 at T4 *p=0.02.

(**e**) Time exploring a mouse throughout trials. Data (means ± SEM) expressed as % of T1 in each group of n=11 eYFP, 7 NpHR3.0 in PVN of *Oxt-CRE* mice. Two-way ANOVA: Interaction of NpHR3.0 stimulation of PVN fibers with light (561nm, continuous stimulation, 5min, ~2mW at T3) and trials: p=0.05, post-hoc Sidak test comparing eYFP with NpHR3.0 at T5 *p=0.015.

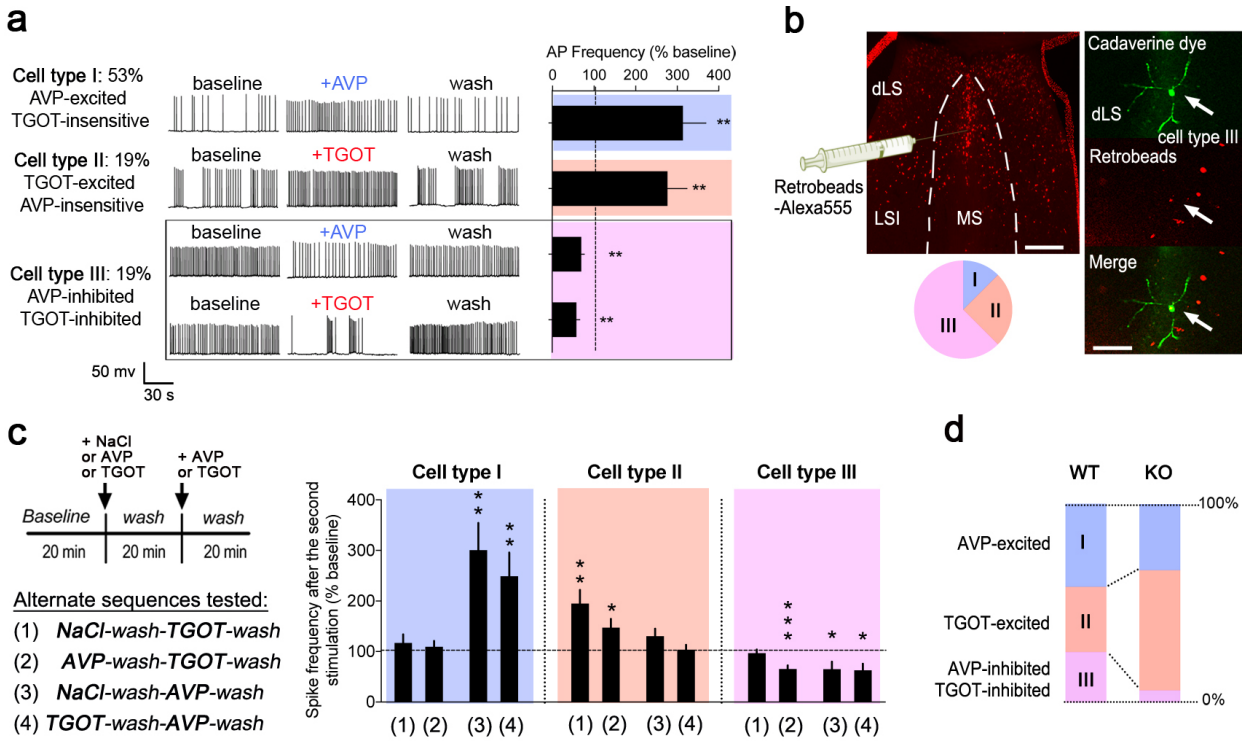

Figure 4. Paucity of cells responding to the orderly sequence of AVP and OXT in LS of *Magel2*$^{+m/-p}$ mice

(**a**) Firing rate of action potentials recorded in whole cell configuration in septal slices at baseline and upon 2-min bath application of AVP (10^{-6} M) and TGOT (10^{-7} M). All 3 types of response reverted to baseline after washout. Data (means±SEM) expressed as % relative to baseline prior treatment in n=29 TGOT-excited, 34 AVP-excited, 20 AVP-inhibited and 16 TGOT-inhibited cells. T-Test for the effect of TGOT-excitation $^{**}p$=0.0007; AVP-excitation $^{**}p$=0.0005; TGOT-inhibition $^{**}p$<0.0001; AVP-inhibition $^{**}p$=0.001.

(**b**) Cells in LSD marked with cadaverine-Alexa-Fluor-594 via the patch pipette corresponded mostly to the type III if they uptake fluorescent retrobeads injected in MS (n=16 neurons, 2 type I, 4 types II, 10 type III in 11 mice). Scales=200 and 50 µm.

(**c**) Effect of orderly sequence of AVP and TGOT on spike frequency. Sequence of 2 stimuli (2 min each) to categorize cell types *a posteriori*. Wilcoxon test for the effect of TGOT alone on type II cells $^{**}p$=0.0027; AVP 1st –TGOT 2nd on type II cells $^{*}p$=0.0155; AVP 1st –TGOT 2nd on type III cells $^{***}p$<0.0001; AVP alone on type I cells $^{**}p$=0.0018; TGOT 1st-AVP 2nd on type I cells $^{**}p$=0.0055; AVP alone on type III cells $^{*}p$=0.039; TGOT 1st-AVP 2nd on type I cells $^{*}p$=0.0138.

(**d**) Proportion of cells categorized as a function of their responses to AVP and TGOT on the frequency of action potentials. n=28WT, 11KO type I cells, 22WT, 20KO type II cells and 17WT, 2KO type III cells in septal slices of 11 *Magel2*$^{+m/-p}$ and 29 WT controls mice.

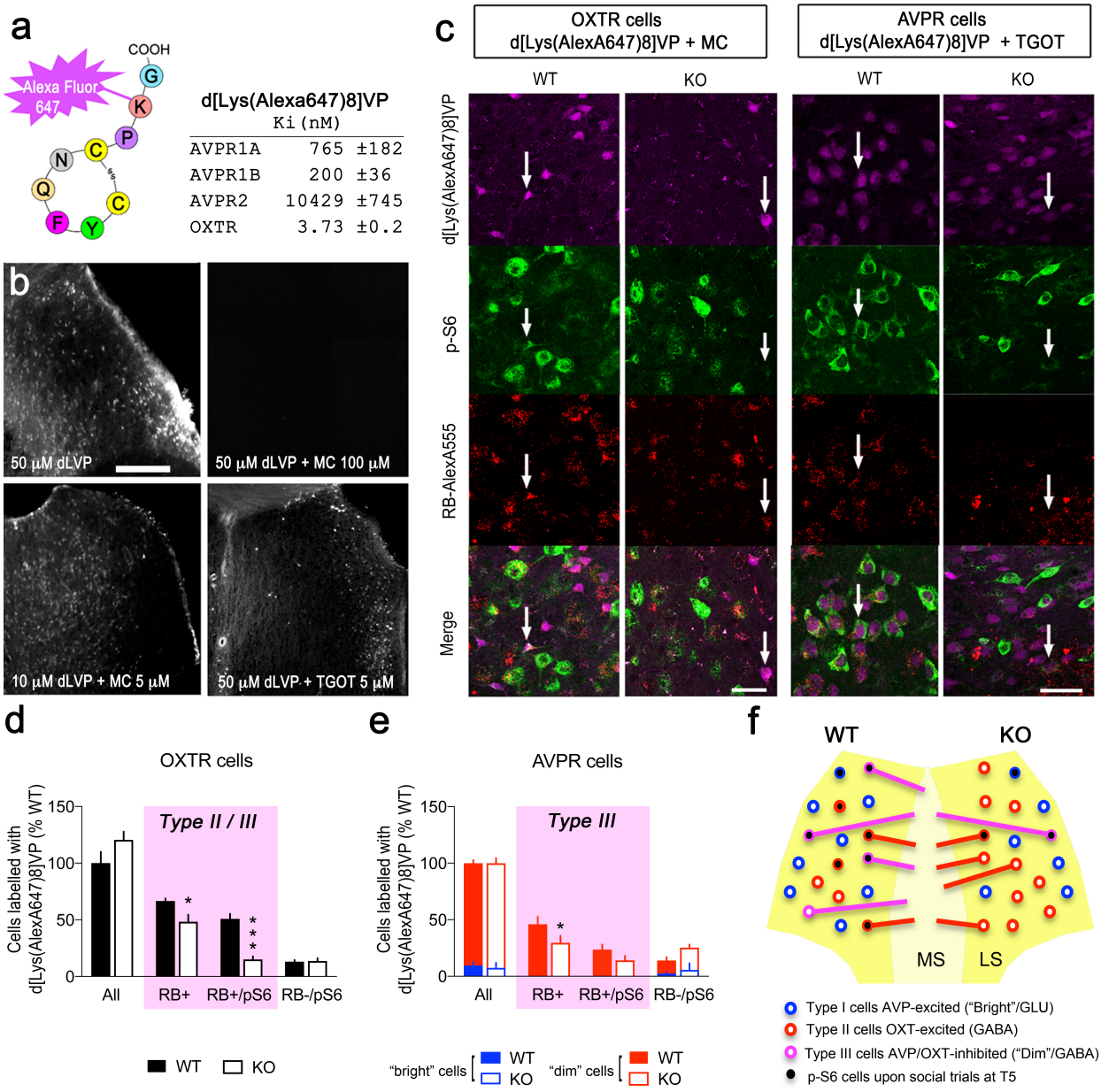

Figure 5. A new fluorescent ligand to identify OXT and AVP responding cells *in vivo*.

(**a**) Affinity of d[Lys(Alexa-Fluor-647)^{8}]VP *in vitro* for the indicated mouse receptors: AVPR1b and OXTR transfected in HEK293 cells and AVPR1a and AVPR2 endogenous from liver and kidney, respectively. Means±SEM of n=3 independent competition assays against [^{3}H]AVP.

(**b**) Representative *in vivo* labeling of cells with intraseptal injection of d[Lys(Alexa-Fluor-647)^{8}]VP in control mice competed entirely when co-injected with the non selective OXTR/AVPR antagonist (100µM MC), and partially with 5µM MC (to block AVPR sites only) or with 5µM TGOT (to block OXTR sites only). Scale=200µm. See the methods for the selectivity of MC and TGOT on mOXTR and mAVPR.

(**c**) Representative *in vivo* labeling of OXTR (left) and AVPR (right) binding sites in LS of WT and *Magel2*$^{+m/-p}$ mice prior injected with retrobeads (RB-Alexa-Fluor-555) in MS to mark cell type III. Cannulated animals were administered with drugs in LS 5min after the last trial of social habitation/discrimination and 10min later, sacrificed. Scale bars=25µm.

(**d**) Percent of cells expressing OXTR binding sites and p-S6 in LS. Total OXTR cells 353WT of which 237RB+, 451KO of which 224RB+. Means±SEM of n=5 WT and 5 *Magel2*$^{+m/-p}$ mice. Two-way ANOVA: Effect of genotype on OXTR cells: $p<0.0001$, post-hoc Sidak test for the percent of OXTR cells projecting to MS *$p=0.0415$ and OXTR cells projecting to MS with pS6 ***$p=0.0002$.
(**e**) Percent of cells expressing AVPR binding sites and p-S6 in LS. Total AVPR cells 474WT of which 235RB+, 379KO of which 112RB+. Means ± SEM of n=5 WT and 5 *Magel2*$^{+m/-p}$ mice. Two-way ANOVA: Effect of genotype on AVPR cells: $p=0.0256$, post-hoc Sidak test for the percent of AVPR cells projecting to MS *$p=0.011$.
(**f**) Summary of cell types equipped with AVPR/ OXTR in LS. Type III cells inhibited by both AVP and TGOT are less solicited (p-S6 signaling) in *Magel2*$^{+m/-p}$ mice compared to WT controls during social trials.

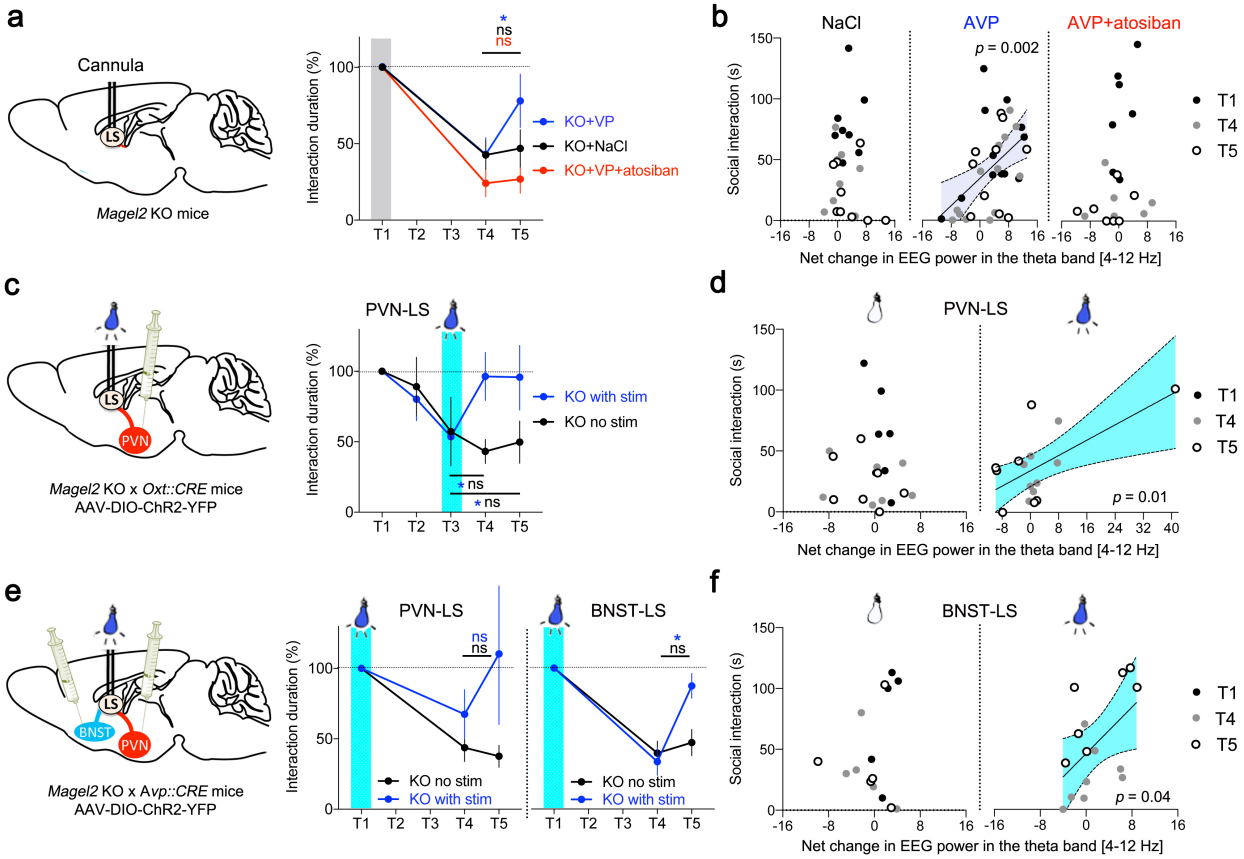

Figure 6. Stimulation of the BNST-LS AVP pathway and PVN-LS OXT pathway restored social behavior in *Magel2*$^{+m/-p}$ mice.

(**a**) Time *Magel2*$^{+m/-p}$ mice explored WT conspecifics after intraseptal injection of AVP (3.10^{-6} M) with or without atosiban (5.10^{-8} M) at T1. Data (means±SEM) expressed as % relative to T1 in each group of n=13NaCl, 12AVP and 6AVP+atosiban mice. Two-way ANOVA: Effect of social trials: $p<0.0001$ post-hoc Dunnett test for the effect of NaCl: T4 vs T1 *$p<0.0001$; effect of AVP: T4 vs T1 *$p<0.0001$ and T4 vs T5 *$p=0.01$; effect of AVP+atosiban: T4 vs T1 *$p<0.0001$.

(**b**) Net changes of EEG power in the theta band between trials correlated with time of social interaction. Pearson coefficient if NaCl injected at T1: $r=-0.08$, $p=0.6$; if AVP injected at T1: $r=0.49$, *$p=0.024$; if AVP+atosiban injected at T1: $r=0.3$, $p=0.18$.

(**c**) Time *Magel2*$^{+m/-p}$ mice explored WT conspecifics after blue light stimulation (473nm, 30Hz, 10ms pulses for 2min, 2mW) of OXT neuron projections between PVN and LS (PVN-LS pathway). Data (means±SEM) expressed as % relative to T1 in each group of n=12 no stim, 12 stim mice. Two-way ANOVA: Effect of ChR2 stim on social trials: $p=0.0037$ post-hoc Dunnett test for the effect of no stim: T3 vs T1 *$p=0.035$; effect of ChR2 stim: T3 vs T1 *$p=0.016$ T3 vs T4 *$p=0.029$ and T3 vs T5 *$p=0.0318$.

(**d**) Net changes of EEG power in the theta band between trials correlated with time of social interaction after optogenetic stimulation of PVN-LS OXT terminals. Pearson coefficient if no stim at T3: $r=-0.2$, $p=0.47$; if ChR2 stim at T3: $r=0.62$, *$p=0.01$.

(**e**) Time *Magel2*$^{+m/-p}$ mice explored WT conspecifics after blue light stimulation (473nm, 20Hz, 5ms pulses for 2min, 2mW) of AVP neuron projections between BNST and LS (BNST-LS pathway) or PVN and LS (PVN-LS pathway). Data (means±SEM) expressed as % relative to T1 in each group of n=9 no stim, 6 stim BNST-LS mice and 9 no stim, 9 stim PVN-LS mice. (Left) Two-way ANOVA: Effect of ChR2 in PVN-LS on social trials: $p=0.2$ post-hoc Dunnett test for the effect of no stim: T4 vs T1 *$p=0.0008$ and T4 vs T5 $p=0.75$; effect of stim: T4 vs T1 $p=0.16$ and T4 vs T5 $p=0.6$. (Right) Two-way ANOVA: Effect of ChR2 in BSNT-LS on social trials: $p=0.005$ post-

hoc Dunnett test for the effect of no stim: T4 vs T1 *p<0.0001 and T4 vs T5 p=0.6; effect of stim: T4 vs T1 *p<0.0001 and T4 vs T5 *p=0.01.

(**f**) Net changes of EEG power in the theta band between trials correlated with time of social interaction. Pearson coefficient if no stim at T1: r=-0.17, p=0.07; if ChR2 stim at T1: r=0.53, *p=0.04.